Application of Proper Orthogonal Decomposition to Analysis of Turbulence Dynamics

David Hatch[1]

Collaborators:

F. Jenko[2], P.W. Terry[3], M.J. Pueschel[3], A. Limone[2], V. Bratanov[2], H. Doerk[2], W.M. Nevins[4], D. del-Castillo Negrete[5]

[1]IFS-UT Austin
[2]IPP-Garching
[3]UW-Madison
[4]Lawrence Livermore National Laboratory
[5]Oak Ridge National Laboratory

Introduction / Motivation

- Turbulence is complex
- POD produces an 'optimal', orthogonal basis for fluctuations
- May be very different from standard representations (i.e. Fourier, orthogonal polynomials, etc.)
- Always more (or equally) efficient than standard representations.
- Terminology:
  - POD, SVD, EOF, PCA

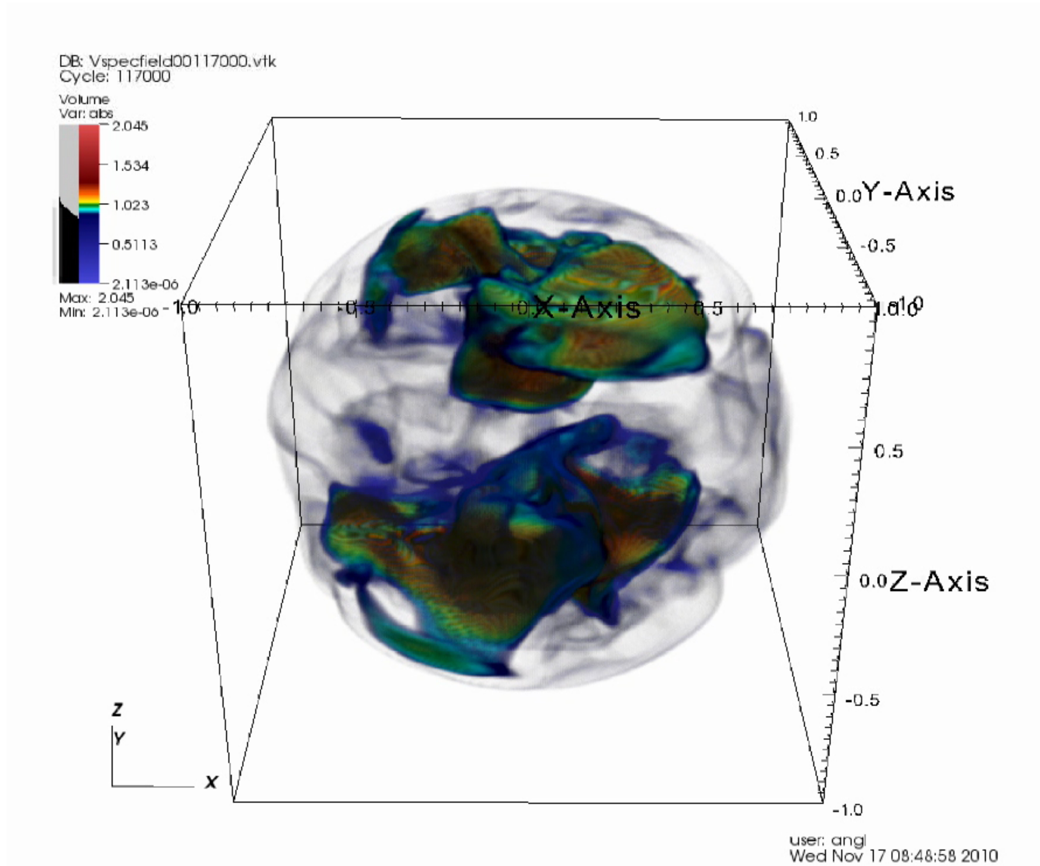

Outline

- SVD-mathematical foundation
  - Orthogonality
  - Optimality
- SVD Applied to turbulence
- Examples
  - Dynamo flows
  - Subdominant microtearing modes
  - Saturation via damped eigenmodes
- Summary/Conclusions

Outline

- **SVD-mathematical foundation**
  - Orthogonality
  - Optimality
- SVD Applied to turbulence
- Examples
  - Dynamo flows
  - Subdominant microtearing modes
  - Saturation via damped eigenmodes
- Summary/Conclusions

Singular Value Decomposition

$$A = U\Sigma V^{\dagger}$$

$A \in \mathbb{C}^{m\times n}$	Input matrix
$U \in \mathbb{C}^{m\times m}$	Columns are **left singular vectors**
$\Sigma \in \mathbb{R}^{m\times n}$	Diagonal (for upper square portion) containing **singular values**
$V \in \mathbb{C}^{n\times n}$	Columns are **right singular vectors**

Singular Value Decomposition

$$AA^{\dagger}U = U\Sigma\Sigma^{\dagger}$$

Left singular vectors are eigenvectors of correlation matrix.

$$A^{\dagger}AV = V\Sigma^{\dagger}\Sigma$$

Right singular vectors are eigenvectors of correlation matrix.

$AA^{\dagger}$ and $A^{\dagger}A$ are Hermitian ➔ U and V are **orthogonal**.

Squared singular values are the eigenvalues (real and positive definite).

SVD-Optimality

SVD as superposition of rank-1 matrices

$$A_{ij} = \sum_{n=1}^{N} \sigma_n u_i^{(n)} v_j^{(n)*}$$

SVD produces the **best possible** rank-r approximation:

$$A_{ij}^{(r)} = \sum_{n=1}^{r<N} \sigma_n u_i^{(n)} v_j^{(n)*}$$

SVD is optimal representation:

Minimizes $\longrightarrow$ $$\epsilon^{(r)} \equiv \frac{||A - A^{(r)}||}{||A^{(r)}||} = \frac{\sum_{n=r+1}^{N} \sigma_n}{\sum_{n=1}^{N} \sigma_n}$$

Outline

- SVD-mathematical foundation
  - Orthogonality
  - Optimality
- **SVD Applied to Turbulence**
- Examples
  - Dynamo flows
  - Subdominant microtearing modes
  - Saturation via damped eigenmodes
- Summary/Conclusions

SVD Applied to Turbulence

$A = U\Sigma V^\dagger \longrightarrow A \in \mathbb{C}^{m\times n}$ Input matrix

$$
\begin{array}{cc}
\begin{array}{c} x_1 \\ x_2 \\ x_3 \\ \cdot \\ \cdot \\ \cdot \end{array} &
\begin{pmatrix} \cdot & \cdot & \cdot & \cdot \\ \cdot & \cdot & \cdot & \cdot \\ \cdot & \cdot & \cdot & \cdot \\ \cdot & \cdot & \cdot & \cdot \end{pmatrix} \\
 & \begin{array}{cccc} t_1 & t_2 & t_3 & \ldots \end{array}
\end{array}
$$

Data=f(**x**,t)

Each column of A is a 'snapshot' in time.

Spatial variation along rows (can be multi-dimensional as long as scalar product is meaningful.

Time variation along columns.

SVD Applied to Turbulence

$$A = U\Sigma V^{\dagger} \longrightarrow U \in \mathbb{C}^{m \times m}$$

Columns are **left singular vectors**

Each column of U is a mode structure.

Ordered from most to least important.

SVD Applied to Turbulence

$$A = U\Sigma V^{\dagger} \longrightarrow V \in \mathbb{C}^{n\times n}$$

Columns are **right singular vectors**

Each column of V is a time amplitude.

Defines how the corresponding mode structure varies in time.

Orthogonality implies uncorrelated in time.

SVD Applied to Turbulence

$$A = U\Sigma V^\dagger \longrightarrow \Sigma \in \mathbb{R}^{m\times n}$$

Diagonal (for upper square portion) containing **singular values**

Squared singular values define how much 'energy' (depending on scalar product) is in each mode.

Outline

- SVD-mathematical foundation
  - Orthogonality
  - Optimality
- SVD Applied to Turbulence
- **Examples**
  - **Dynamo flows**
  - Subdominant microtearing modes
  - Saturation via damped eigenmodes
- Summary/Conclusions

Madison Dynamo Experiment

MDE—designed to produce Dudley-James flow

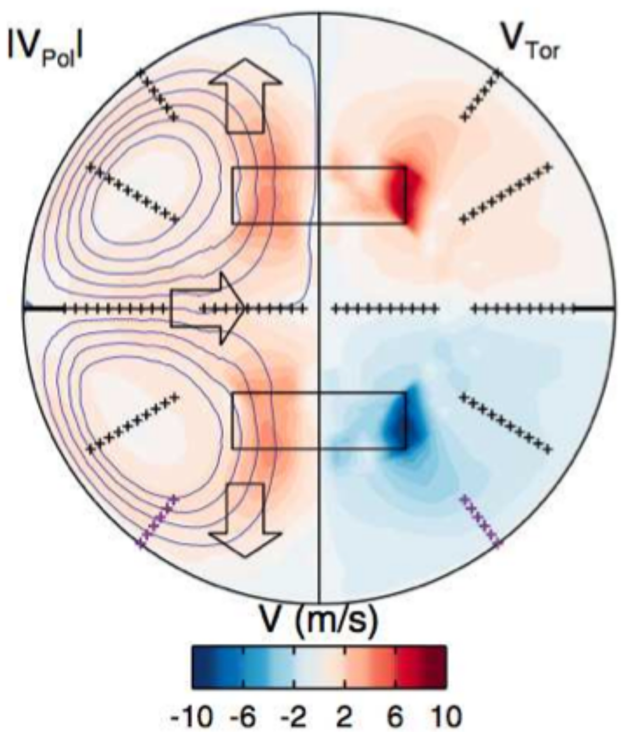

A. Limone

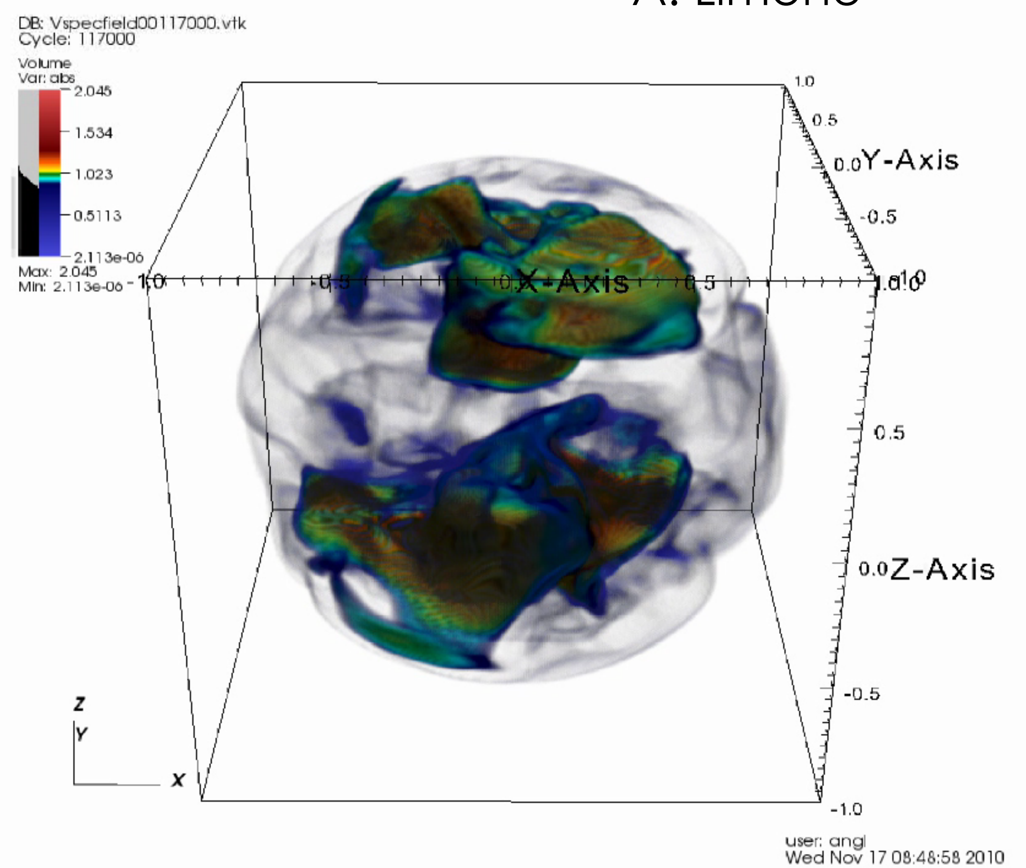

POD n=1: Dudley-James Flow

$$A_{ij} = \sum_{k=1}^{N_{\mathrm{SVD}}} \sigma_k u_k(\mathbf{r}_i) v_k(t_j)$$

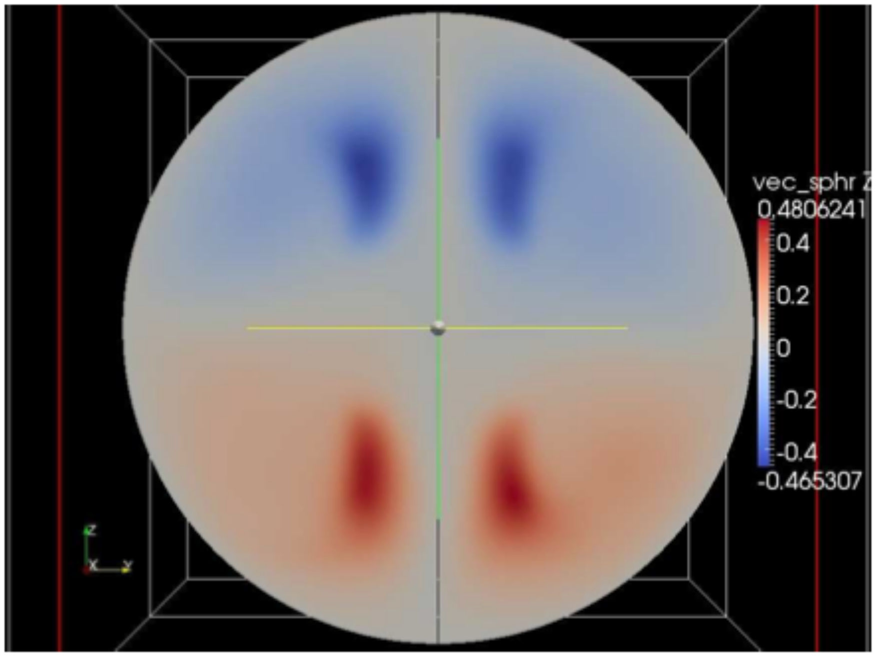

Figure 5: First SVD eigenfunction, $Re_0 = 600$: The color represents the magnitude of the ϕ-component of the field.

First POD mode = Dudley-James flow

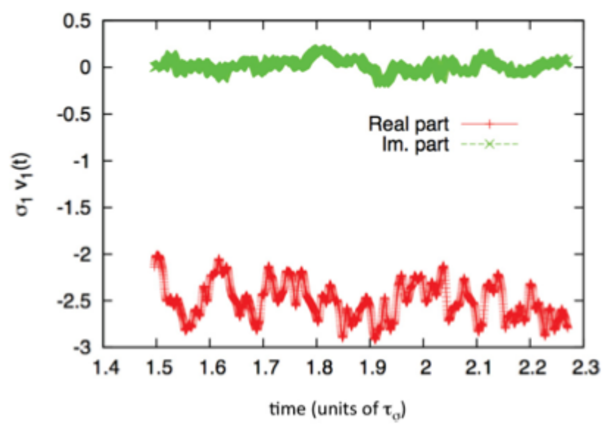

A. Limone et al., PRE, 2012.

POD n=2

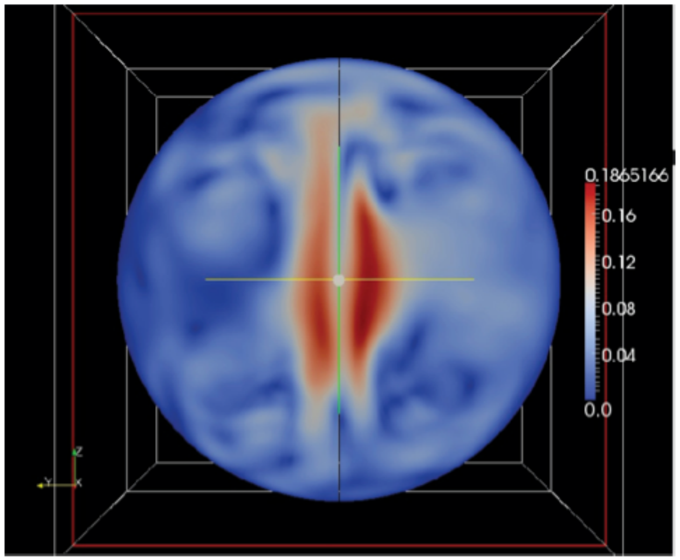

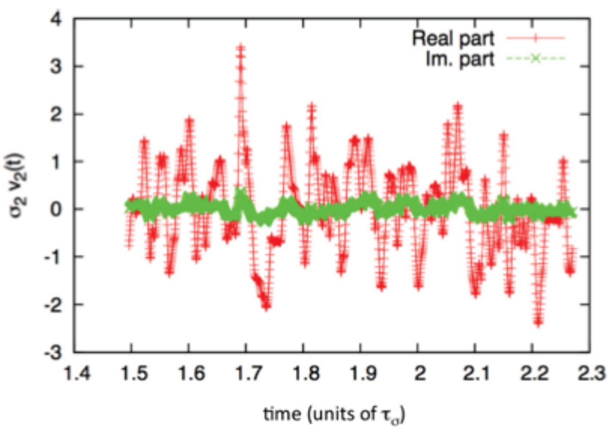

Second POD mode:

Helical flow around axis.

Vertical orientation violates symmetry of impellers?

Not easily characterized in terms of a few spherical harmonics.

POD time trace➔Symmetry maintained on time average.

A. Limone et al., PRE, 2012.

POD n=2 suppresses dynamo

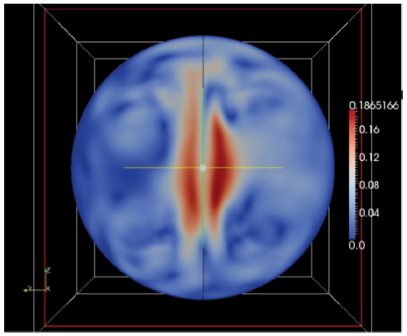

POD n=2 suppresses dynamo growth rates.

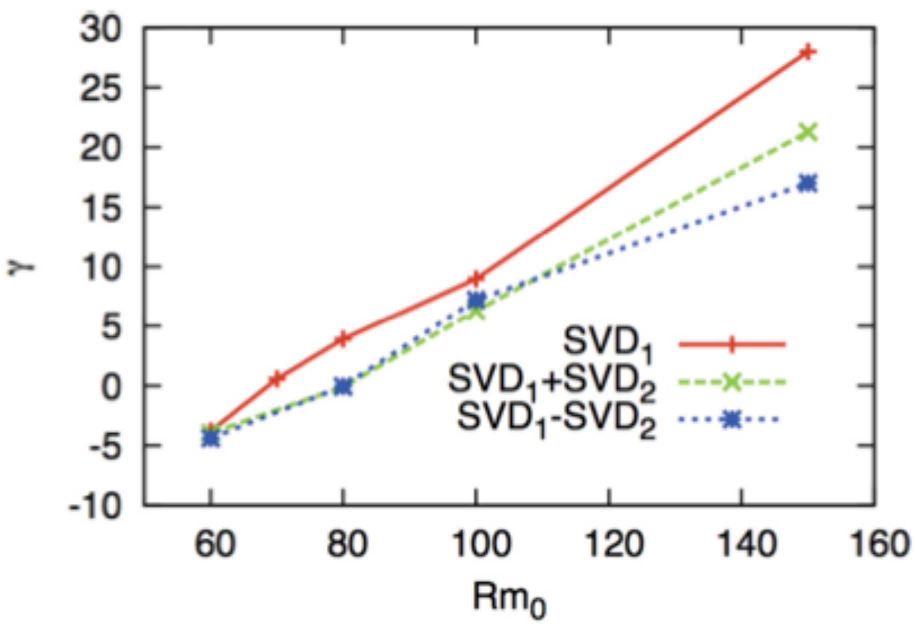

TABLE III. Kinematic simulations of dynamos with an implemented equatorial disk in the center of the equatorial plane. γ_d is the growth rate (the time is scaled to the resistive diffusion time, $\tau_\sigma = \mu_0 \sigma L^2$) of E_M in the presence of the disk; γ_r is the growth rate in the presence of the ring; and γ_0 is the default growth rate, i.e., without any baffle.

Re_0	Rm_0	l_{max}	r_d	γ_r	γ_d	γ_0
300	80	30	0.28	7.62	18.8	4
300	100	30	0.28	15.5	30.8	9.8
300	150	30	0.28	31.2	58.6	24
300	250	30	0.28	52	109	39
600	250	52	0.28	28.4	45.4	22.6
600	250	72	0.28	29.9	50.4	22.6
1000	300	52	0.65	10.4	18.4	10.4

Simulations indicate that a disk designed to suppress POD mode 2 may facilitate dynamo.

Experimental implementation in progress?

A. Limone et al., PRE, 2012.

Outline

- SVD-mathematical foundation
  - Orthogonality
  - Optimality
- **Examples**
  - Dynamo flows
  - **Subdominant microtearing modes**
  - Saturation via damped eigenmodes
- Summary/Conclusions

Electromagnetic Transport

- ITG driven turbulence [Candy PoP '05, Pueschel PoP '08]:
- Levels of electron electromagnetic heat transport that approach electrostatic transport as beta increases.
- Magnetic Stochasticity observed

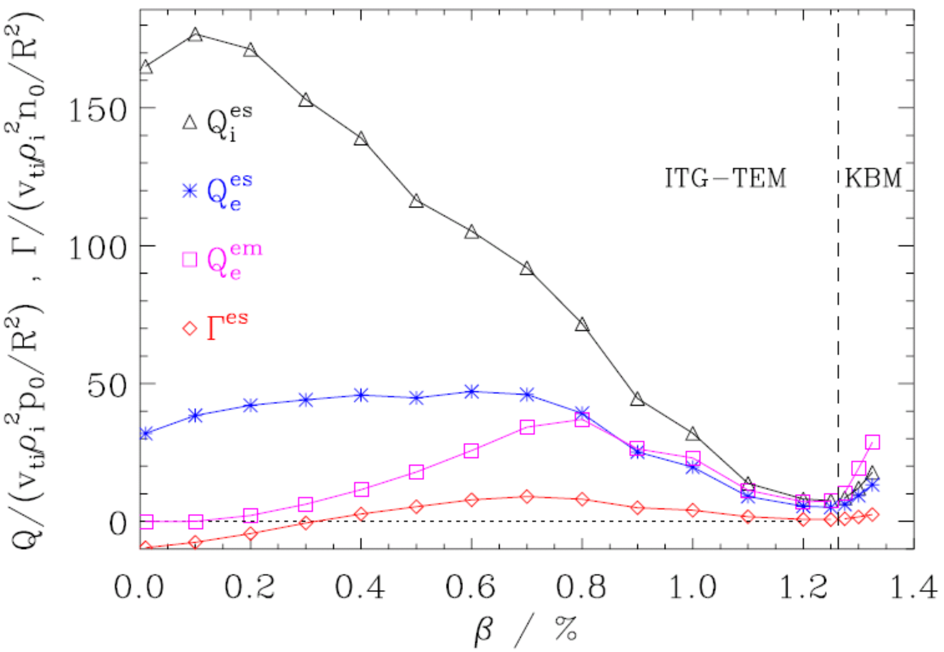

Pueschel, PoP, '08

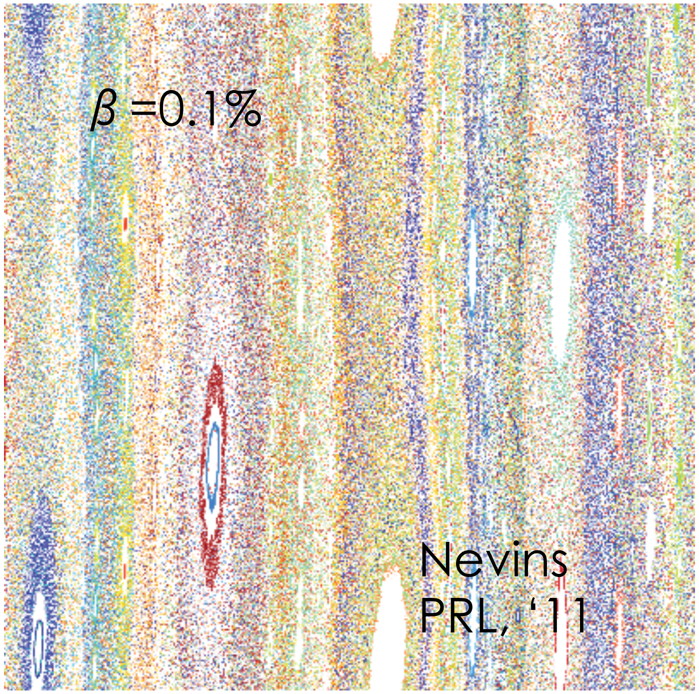

Nevins PRL, '11

Tearing Parity

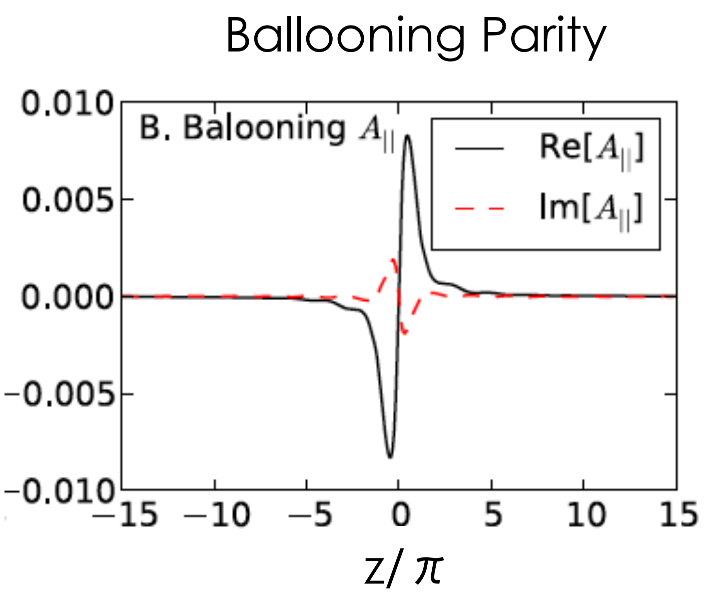

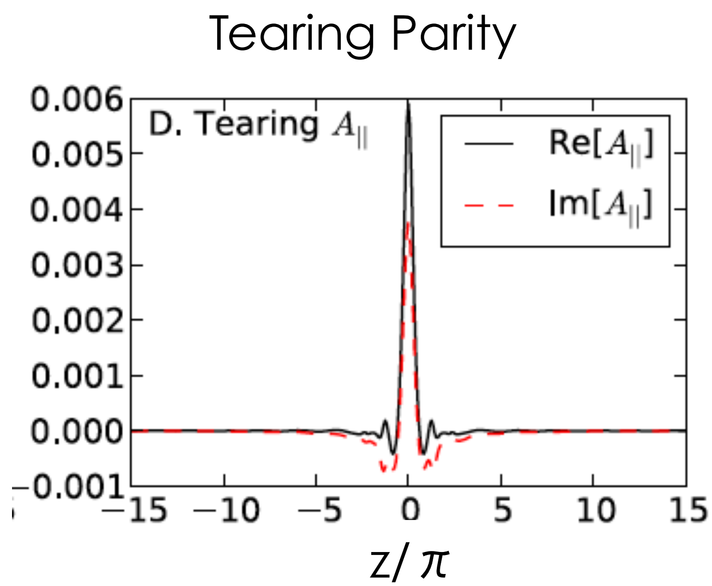

Resonant component extracted by integral along field line.
➔ITG has no resonant component (at kx=0).
➔Tearing parity is resonant.

$$A_{||}^{res} = \int A_{||}(x = x_{res}(k_y), k_y, z)dz$$

What is the cause of stochasticity and EM transport?

$A_{||}$ Mixed Parity in Nonlinear

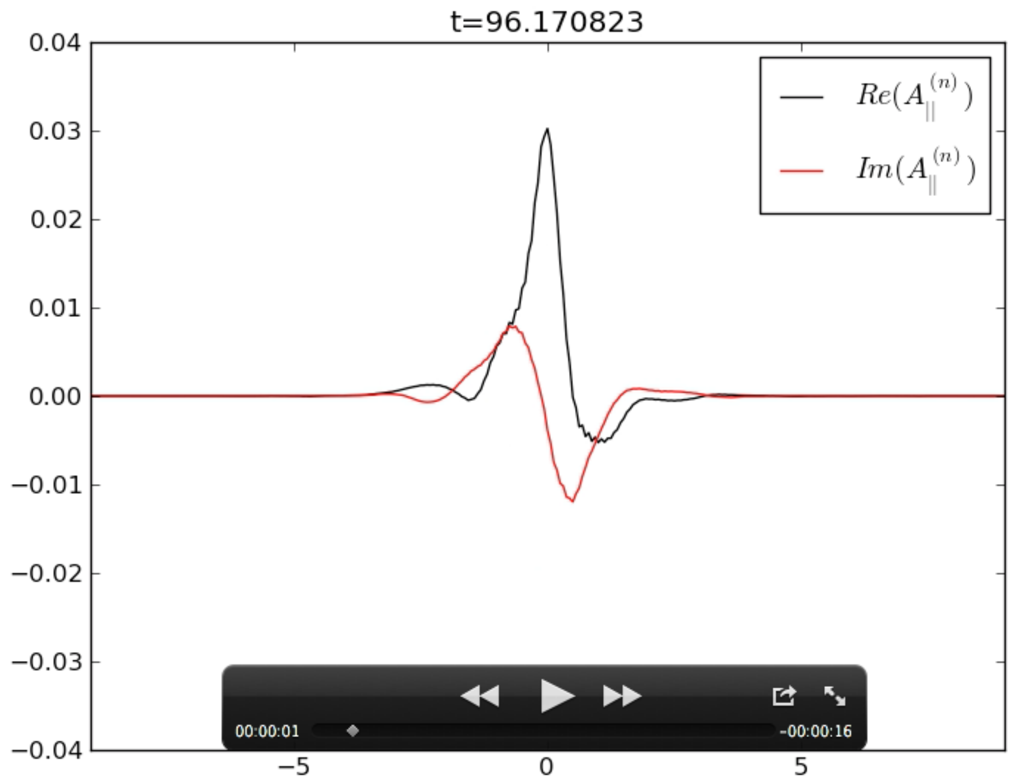

Simulations: GENE code (gene.rzg.mpg.de)

Fluctuations Captured With Two Modes

First two POD modes:
One has ballooning parity (ITG)
One has tearing parity.

Two modes capture almost all of important effects

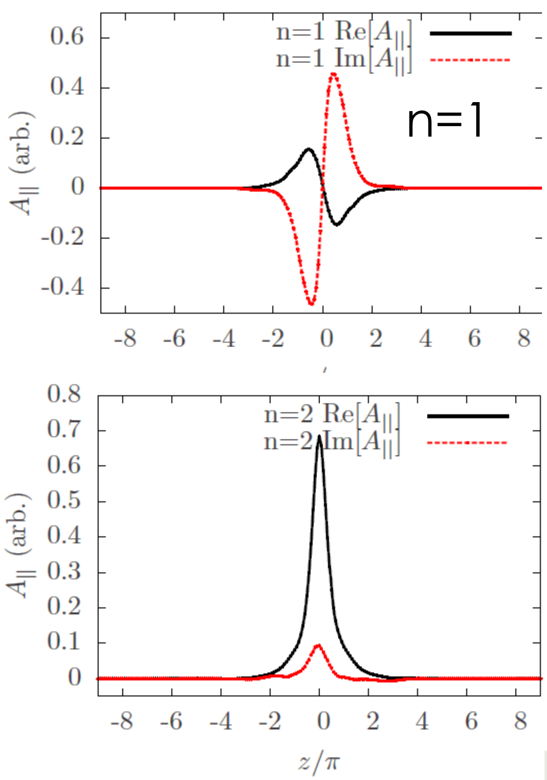

Distinct Transport Mechanisms at Same Scales

$$A_{\|k_x,k_y}(z,t) = A^{(ball)}_{\|k_x,k_y}(z,t) + A^{(tear)}_{\|k_x,k_y}(z,t) + A^{(res)}_{\|k_x,k_y}(z,t) \left\{ \begin{array}{l} Q_e^{EM\,(tot)} = q_{e\|} B_x / B_0 \\ Q_e^{EM\,(tear)} = q_{e\|} B_x^{(tear)} / B_0 \\ Q_e^{EM\,(ball)} = q_{e\|} B_x^{(ball)} / B_0 \\ Q_e^{EM\,(res)} = q_{e\|} B_x^{(res)} / B_0 \end{array} \right.$$

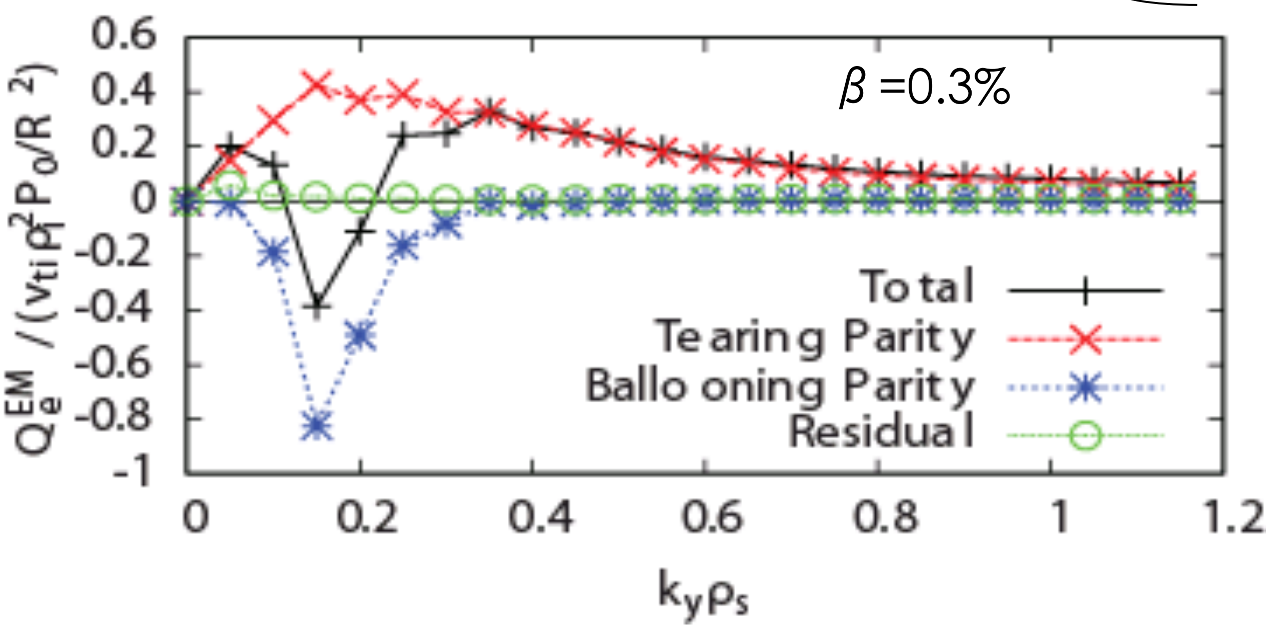

Comparison of SVD mode and linear eigenmodes➔ **This is a nonlinear manifestation of a linearly stable microtearing mode.**

D.R. Hatch et al., PRL 2012., PoP 2013.

Outline

- SVD-mathematical foundation
  - Orthogonality
  - Optimality
- **Examples**
  - Dynamo flows
  - Subdominant microtearing modes
  - **Saturation via damped eigenmodes**
- Summary/Conclusions

Gyrokinetics--Energetics

Gyrokinetic free energy equation:

$$\frac{\partial E}{\partial t} = Q + C$$

Energy sink C ➔ collisional dissipation (negative definite)

Energy source Q proportional to heat flux)

Saturation Through Damped Eigenmodes

$$\frac{\partial E}{\partial t} = Q + C$$

Energy sink C ➔ collisional dissipation

Energy source Q proportional to heat flux

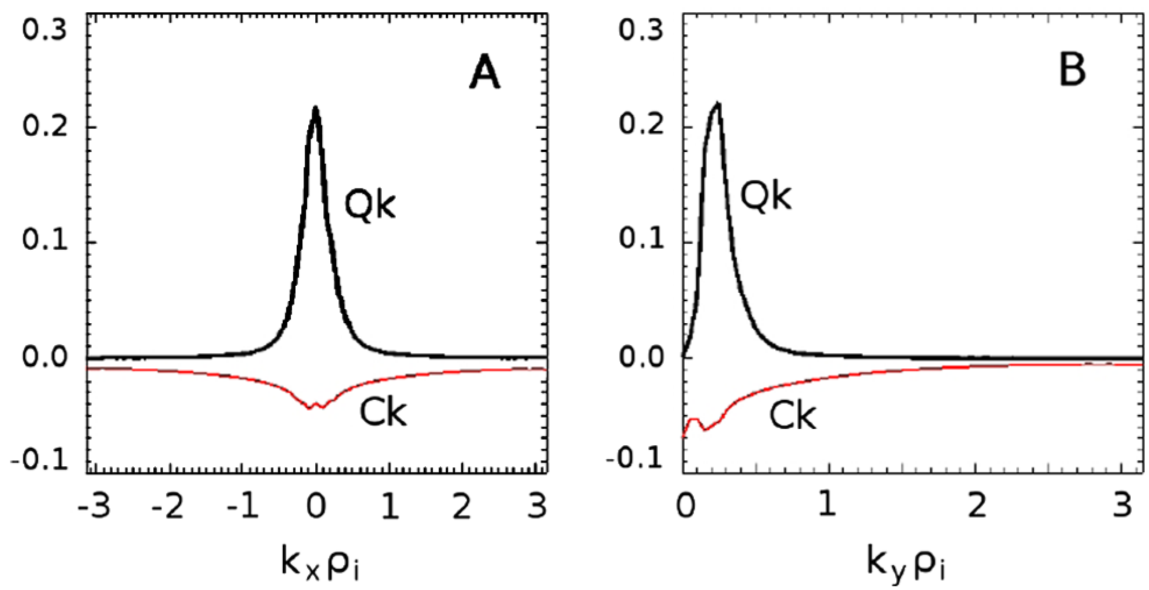

--Cyclone Base Case ITG (and everything else we've looked at): Significant dissipation in region of instability (Hatch et al. PRL 2011).

--Damped modes nonlinearly driven at same scales as ITG

➔What modes are responsible?

Damped Eigenmodes in Simple System

- Goal: examine simple system in order to identify damped eigenmodes
  - Slab ITG
  - Adiabatic electrons
  - Integrated over perpendicular velocity
  - Model similar to Watanabe, Sugama PoP '04 (but we keep range of kz)
- Examine three levels
  - Linear spectra
  - Pseudospectra—bridge between linear and nonlinear
  - Nonlinear--SVD

DNA Code

DNA code:
Direct Numerical Analysis
of Fundamental Gyrokinetic Turbulence Dynamics

Fully Spectral:
Fourier in three spatial dimensions
Hermite in parallel velocity

Developed from scratch, but much of the structure and many algorithms inspired and informed by GENE.

Linear Operator – Matrix Representation

Linear operator in Hermite representation:

$$L = -ik_z\sqrt{1/2}\begin{pmatrix} 0 & \sqrt{1} & 0 & 0 & \cdots \\ \sqrt{2}\pi^{-\frac{1}{4}}e^{-k_\perp^2}D(k_\perp)+\sqrt{1} & 0 & \sqrt{2} & 0 & 0 \\ 0 & \sqrt{2} & 0 & \sqrt{3} & 0 \\ 0 & 0 & \sqrt{3} & 0 & \sqrt{4} \\ \vdots & 0 & 0 & \sqrt{4} & \ddots \end{pmatrix}$$

$$-\nu\begin{pmatrix} 0 & 0 & 0 & 0 & \cdots \\ 0 & 1 & 0 & 0 & 0 \\ 0 & 0 & 2 & 0 & 0 \\ 0 & 0 & 0 & 3 & 0 \\ \vdots & 0 & 0 & 0 & \ddots \end{pmatrix} \qquad +ik_y e^{-k_\perp^2}\pi^{-1/4}D(k_\perp)\begin{pmatrix} \omega_T k_\perp^2/2-\omega_n & 0 & 0 & 0 & \cdots \\ 0 & 0 & 0 & 0 & 0 \\ \omega_T/\sqrt{2} & 0 & 0 & 0 & 0 \\ 0 & 0 & 0 & 0 & 0 \\ \vdots & 0 & 0 & 0 & \ddots \end{pmatrix}$$

Linear Spectra

	No Collisions	Collisions
No Gradient	X	
Gradient		

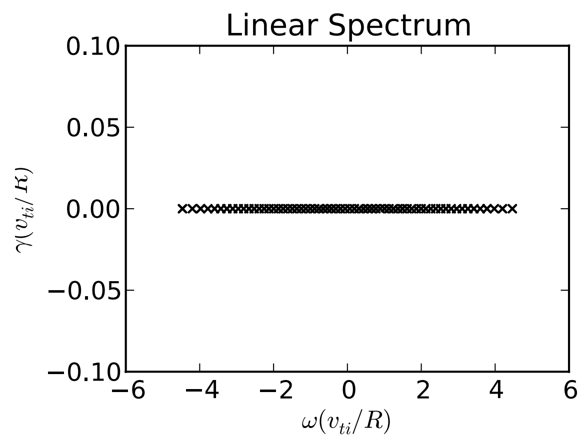

$$L = -ik_z\sqrt{1/2}\begin{pmatrix} 0 & \sqrt{1} & 0 & 0 & \cdots \\ \sqrt{2}\pi^{-\frac{1}{4}}e^{-k_\perp^2}D(k_\perp)+\sqrt{1} & 0 & \sqrt{2} & 0 & 0 \\ 0 & \sqrt{2} & 0 & \sqrt{3} & 0 \\ 0 & 0 & \sqrt{3} & 0 & \sqrt{4} \\ \vdots & 0 & 0 & \sqrt{4} & \ddots \end{pmatrix}$$

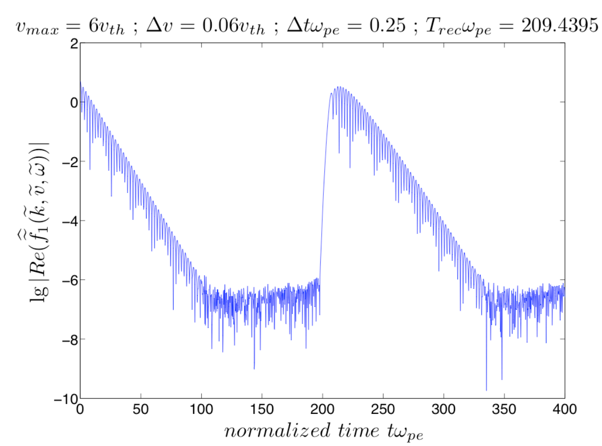

Case, Van Kampen

Linear Spectra

	No Collisions	Collisions
No Gradient		X
Gradient		

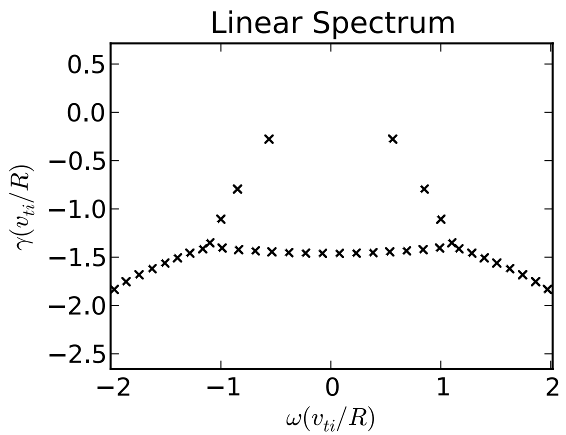

$$L = -ik_z\sqrt{1/2}\begin{pmatrix} 0 & \sqrt{1} & 0 & 0 & \cdots \\ \sqrt{2}\pi^{-\frac{1}{4}}e^{-k_\perp^2}D(k_\perp)+\sqrt{1} & 0 & \sqrt{2} & 0 & 0 \\ 0 & \sqrt{2} & 0 & \sqrt{3} & 0 \\ 0 & 0 & \sqrt{3} & 0 & \sqrt{4} \\ \vdots & 0 & 0 & \sqrt{4} & \ddots \end{pmatrix} \quad -\nu\begin{pmatrix} 0 & 0 & 0 & 0 & \cdots \\ 0 & 1 & 0 & 0 & 0 \\ 0 & 0 & 2 & 0 & 0 \\ 0 & 0 & 0 & 3 & 0 \\ \vdots & 0 & 0 & 0 & \ddots \end{pmatrix}$$

(Skiff et al. PRL ’98, Ng et al. PRL ’99)

Linear Spectra

	No Collisions	Collisions
No Gradient		
Gradient	X	

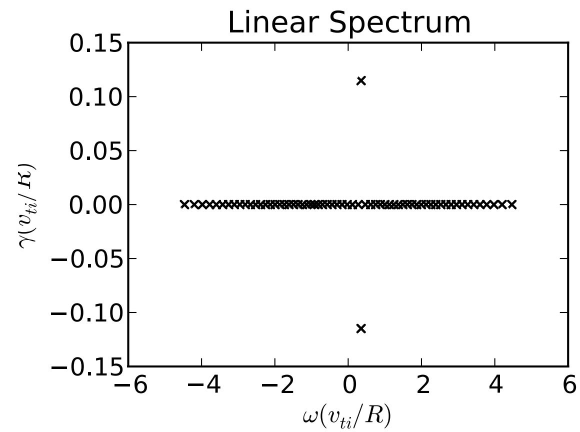

$$L = -ik_z\sqrt{1/2}\begin{pmatrix} 0 & \sqrt{1} & 0 & 0 & \cdots \\ \sqrt{2}\pi^{-\frac{1}{4}}e^{-k_\perp^2}D(k_\perp)+\sqrt{1} & 0 & \sqrt{2} & 0 & 0 \\ 0 & \sqrt{2} & 0 & \sqrt{3} & 0 \\ 0 & 0 & \sqrt{3} & 0 & \sqrt{4} \\ \vdots & 0 & 0 & \sqrt{4} & \ddots \end{pmatrix}$$
$$+ik_y e^{-k_\perp^2}\pi^{-1/4}D(k_\perp)\begin{pmatrix} \omega_T k_\perp^2/2-\omega_n & 0 & 0 & 0 & \cdots \\ 0 & 0 & 0 & 0 & 0 \\ \omega_T/\sqrt{2} & 0 & 0 & 0 & 0 \\ 0 & 0 & 0 & 0 & 0 \\ \vdots & 0 & 0 & 0 & \ddots \end{pmatrix}$$

Linear Spectra

	No Collisions	Collisions
No Gradient		
Gradient		X

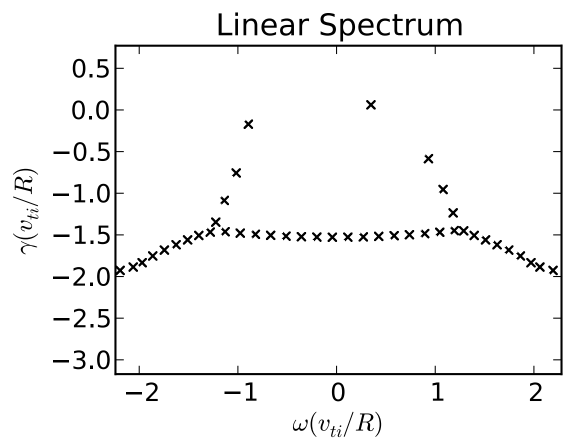

$$L = -ik_z\sqrt{1/2}\begin{pmatrix} 0 & \sqrt{1} & 0 & 0 & \cdots \\ \sqrt{2}\pi^{-\frac{1}{4}}e^{-k_\perp^2}D(k_\perp)+\sqrt{1} & 0 & \sqrt{2} & 0 & 0 \\ 0 & \sqrt{2} & 0 & \sqrt{3} & 0 \\ 0 & 0 & \sqrt{3} & 0 & \sqrt{4} \\ \vdots & 0 & 0 & \sqrt{4} & \ddots \end{pmatrix}$$

$$+ik_y e^{-k_\perp^2}\pi^{-1/4}D(k_\perp)\begin{pmatrix} \omega_T k_\perp^2/2-\omega_n & 0 & 0 & 0 & \cdots \\ 0 & 0 & 0 & 0 & 0 \\ \omega_T/\sqrt{2} & 0 & 0 & 0 & 0 \\ 0 & 0 & 0 & 0 & 0 \\ \vdots & 0 & 0 & 0 & \ddots \end{pmatrix} \quad -\nu\begin{pmatrix} 0 & 0 & 0 & 0 & \cdots \\ 0 & 1 & 0 & 0 & 0 \\ 0 & 0 & 2 & 0 & 0 \\ 0 & 0 & 0 & 3 & 0 \\ \vdots & 0 & 0 & 0 & \ddots \end{pmatrix}$$

Linear Eigenmodes - Properties

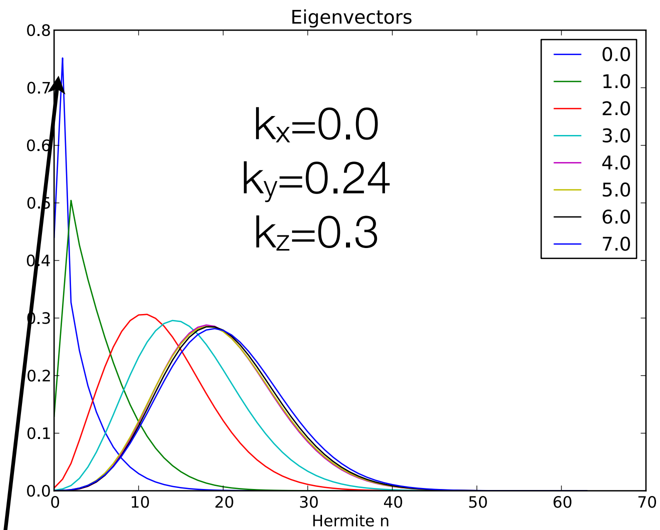

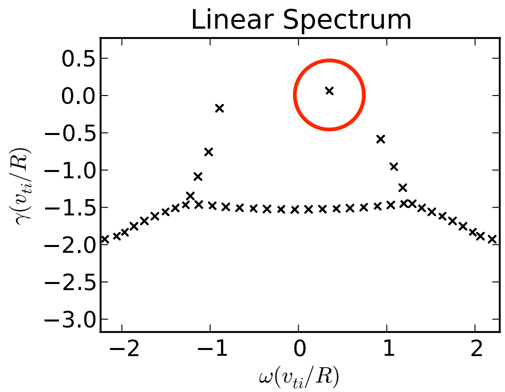

ITG mode:
Relation between f0 and f2 ==> **large drive**
smooth velocity space structure (low order Hermites):
low collisionality

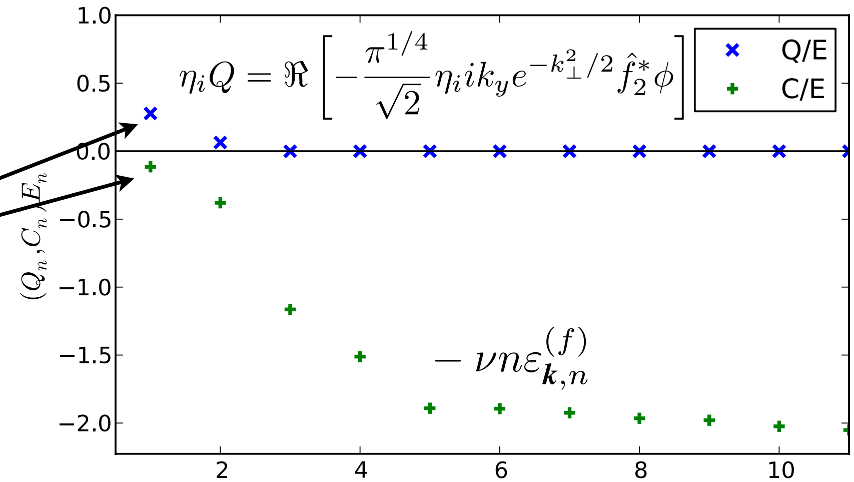

Eigenmode number

Linear Eigenmodes - Properties

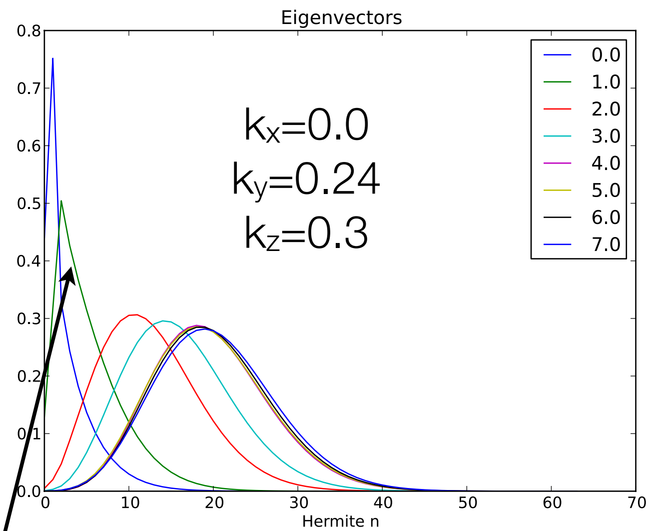

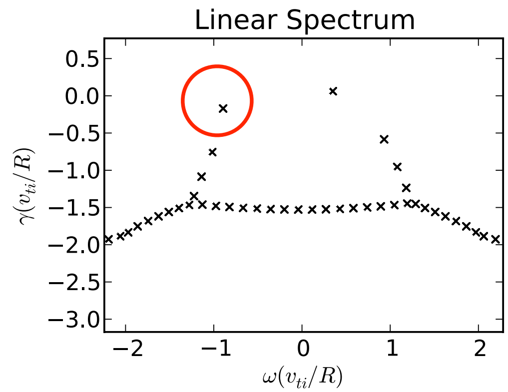

Drift Wave:
Relation between f0 and f2 ==> **moderate drive**
smooth velocity space structure (low order Hermites):
low collisionality

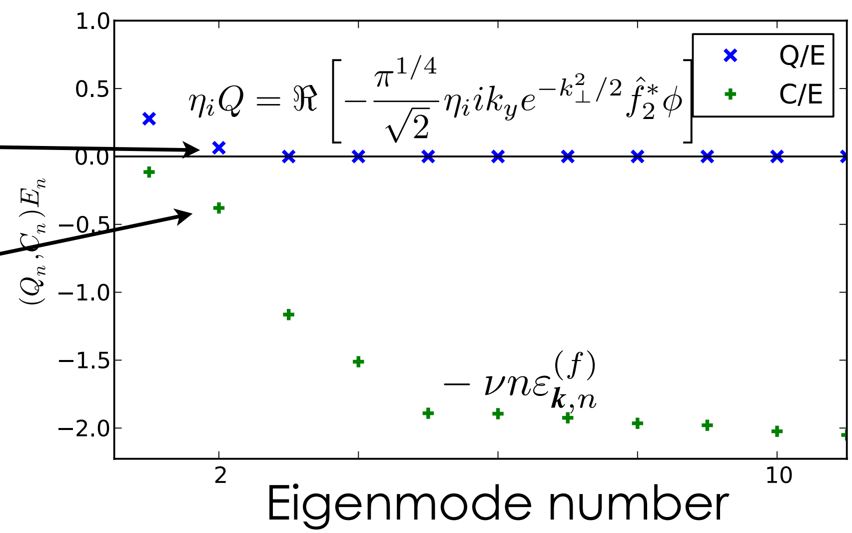

Linear Eigenmodes - Properties

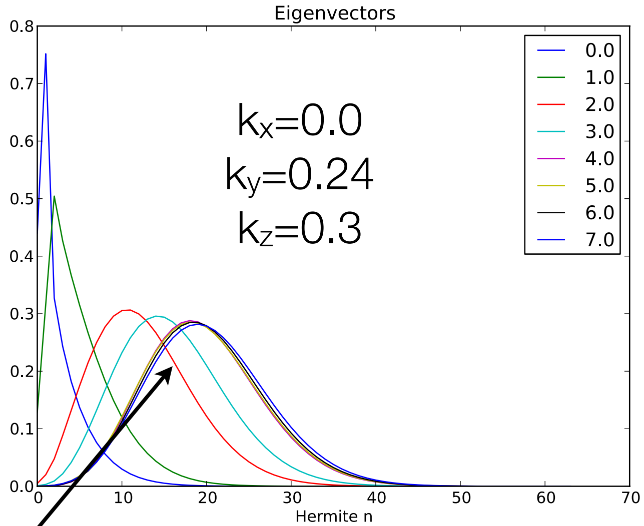

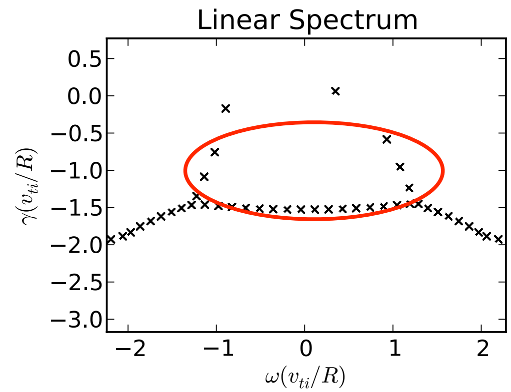

Landau roots:
Relation between f0 and f2 ==> **virtually 0**
smooth velocity space structure (low order Hermites):
high collisionality

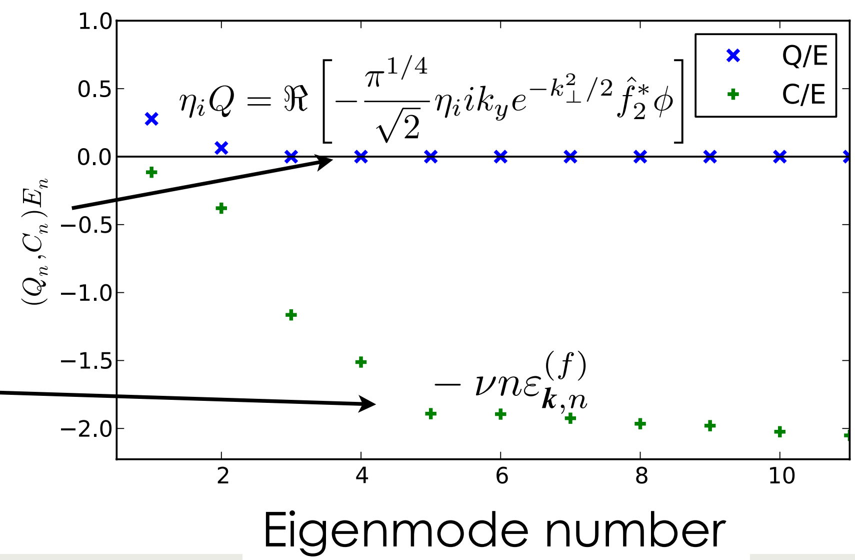

Pseudospectrum – Slab ITG

$$\Lambda_\epsilon(A) \;=\; \{\, z \in \mathbf{C} : \;\|(zI - A)^{-1}\| \geq \epsilon^{-1}$$

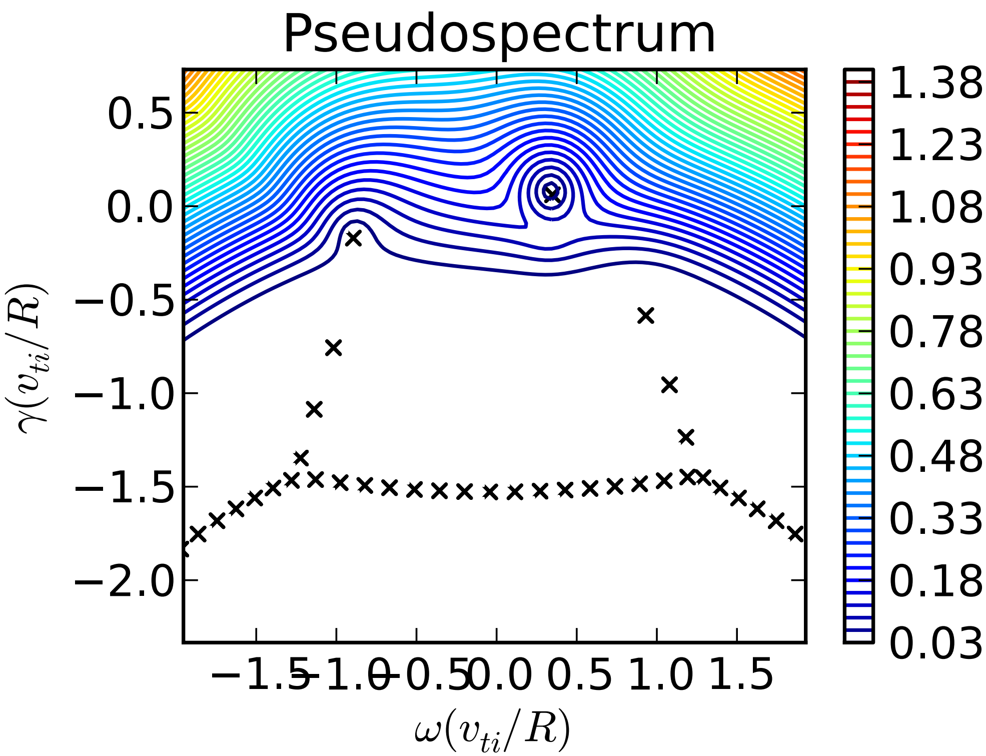

Closely nested surfaces around ITG mode (and to a lesser extent around DW.

Pseudospectra—Trefethen, SIAM review, 1997.

Pseudospectrum – Slab ITG

$$\Lambda_\epsilon(A) = \{ z \in \mathbf{C} : \; \|(zI - A)^{-1}\| \geq \epsilon^{-1}$$

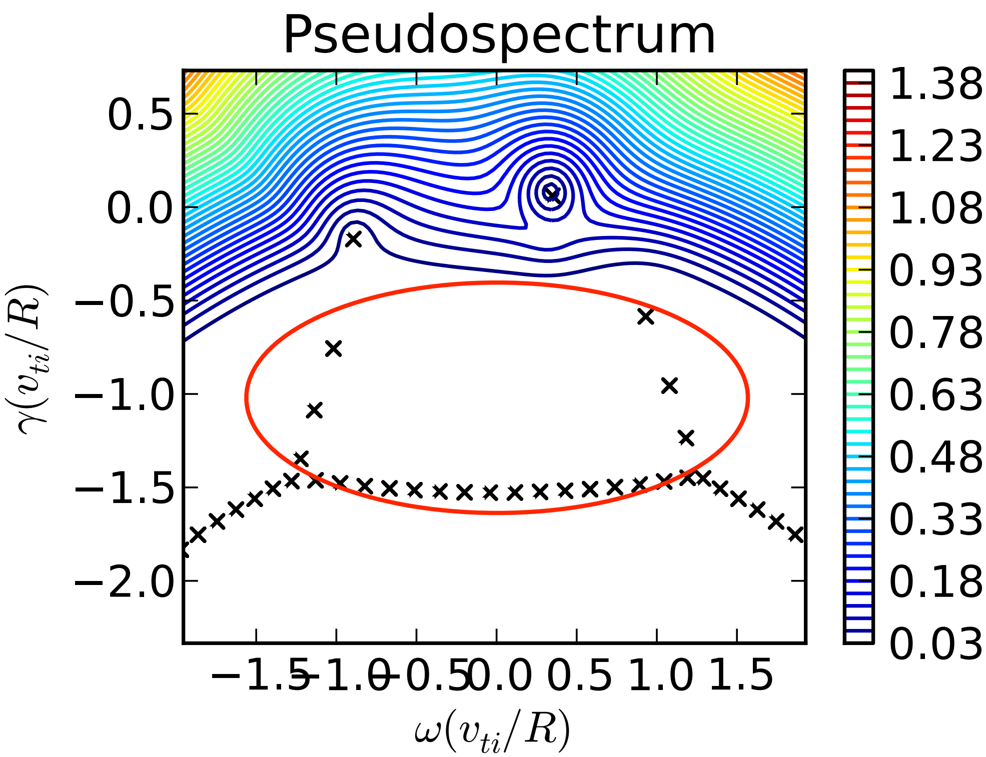

Highly non-orthogonal in this region

All frequencies in this region are highly resonant

Would not expect fluctuations to match eigenvalues here.

Direct Eigenmode Decompostion Infeasible

- Case-Van Kampen emphasized that eigenmodes form complete basis (even though they are nonorthogonal)
- Eigenvectors of adjoint operator serve as projection operators
- In practice nonorthogonality is too extreme==>cannot associate any quadratic quantity (e.g. free energy or heat flux) uniquely with individual eigenmodes.

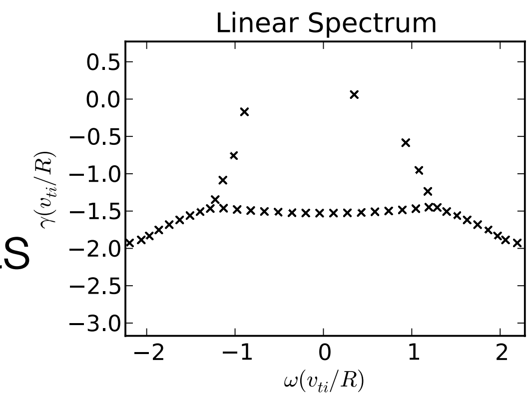

Use SVD to Extract Optimal Modes

Take distribution (for certain kx,ky,kz) from nonlinear dataset, and construct SVD:

$$\hat{f}_n(t) = \sum_s \sigma_s \hat{g}_n^{(s)} h^{(s)}(t)$$

σ_s =singular value--average amplitude

$\hat{g}_n^{(s)}$ and $h^{(s)}(t)$ are orthonormal and 'optimal' (rigorously more efficient than any other decomposition)

Pseudo-eigenvalues From SVD Modes

Already Noted: direct projection onto linear eigenmodes is meaningless

Go backwards from SVD:

Get 'pseudo-eigenvalues' by minimizing $||A\hat{g}_n - z\hat{g}_n||$ over the complex plane for a given SVD mode g_n

This is zero for an exact eigenvector

pseudo-eigenvalue is the location in the complex plane where $||A\hat{g}_n - z\hat{g}_n||$ is minimized

Nonlinear spectra

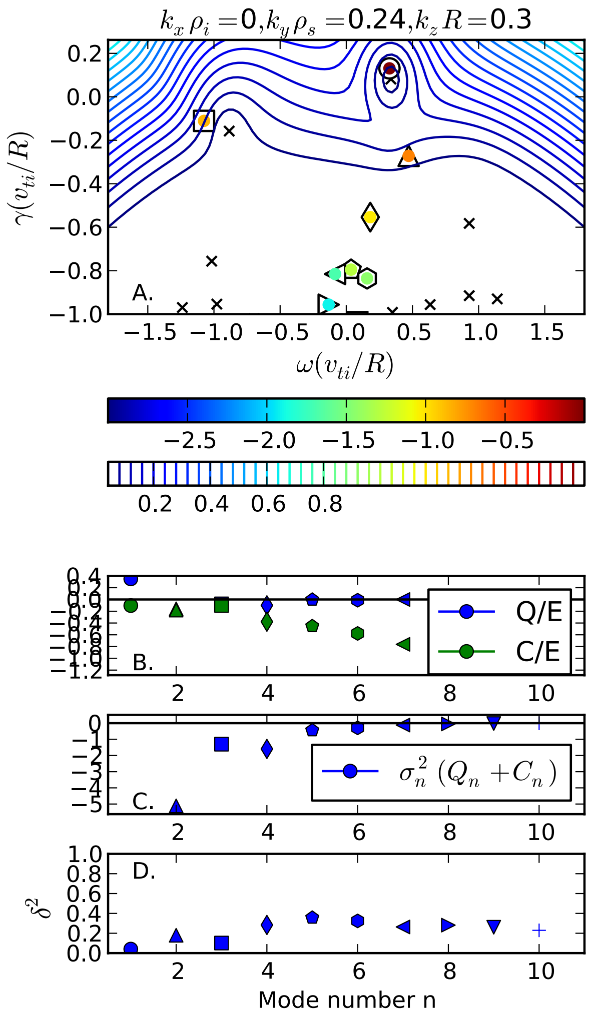

Combine information
- -linear
- -pseudospectra
- -nonlinear

Mode growth/damping rates for Q and C

Net damping rate (including amplitude)

How close to being an eigenvalue

Nonlinear spectra

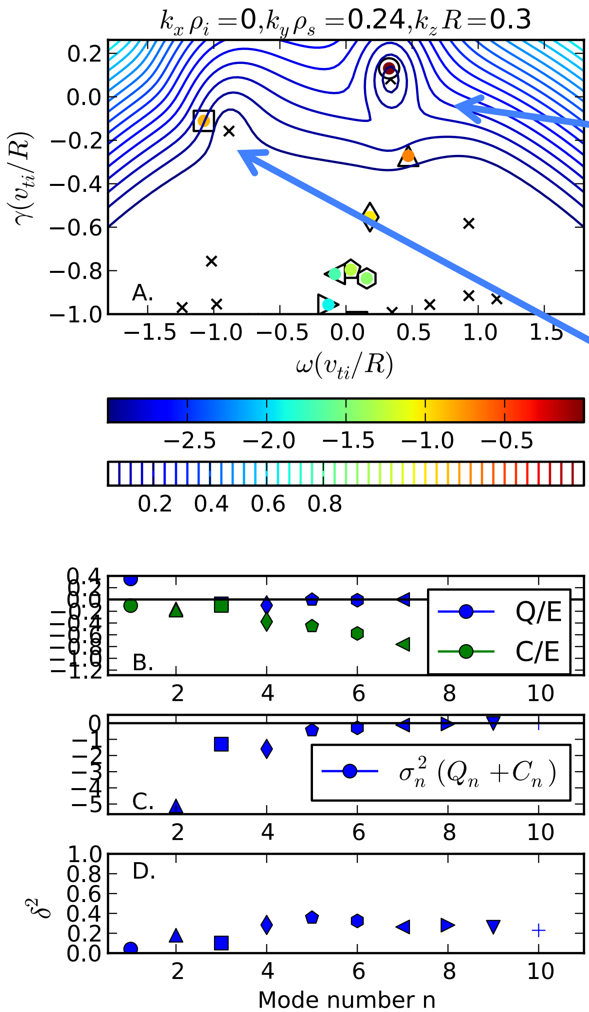

ITG

DW

ITG and DW clearly identified.

ITG and DW clearly identified.

Nonlinear spectra

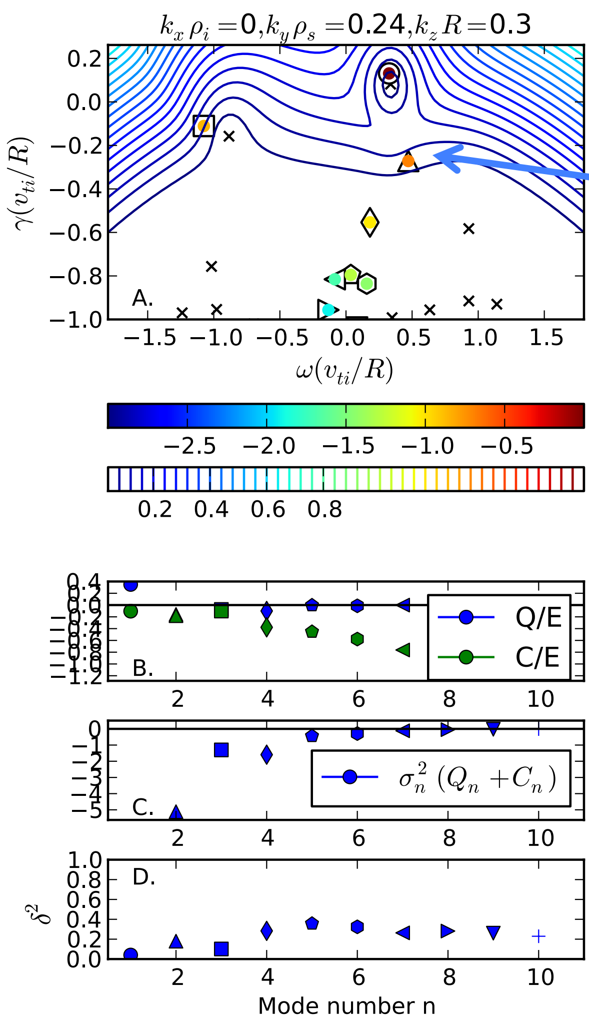

Typically one or more modes with negative Q—i.e., inward heat flux. Significant energy sink.

Dissimilar to anything in the linear spectrum.

Landau-like roots don't play big role (at low k).

Negative Q Mode in Pseudospectrum

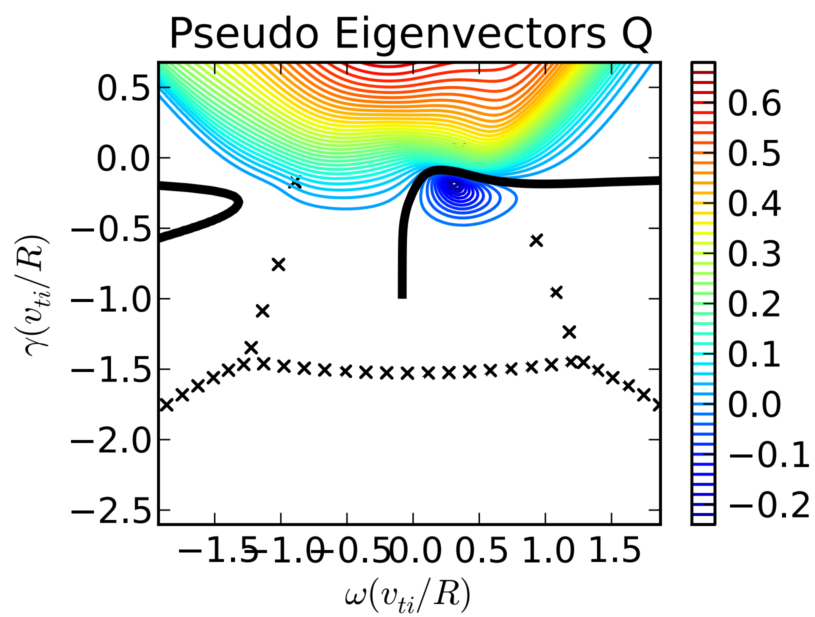

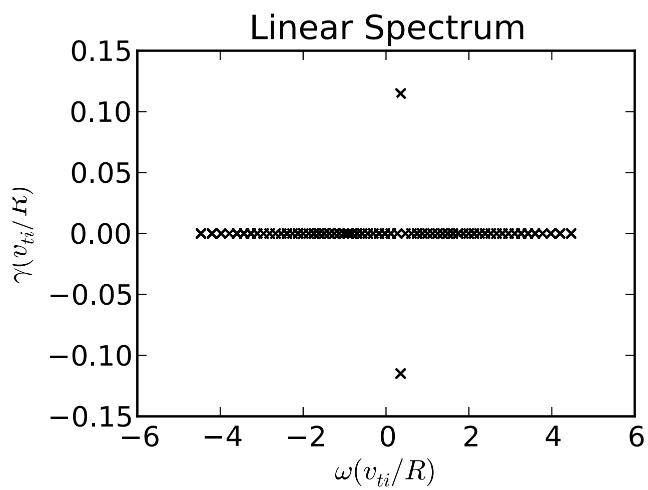

Negative Q is still observed in pseudo spectrum
Same region as mirror mode in collisionless linear spectrum!

Damped Modes – Significant Net Energy Sink

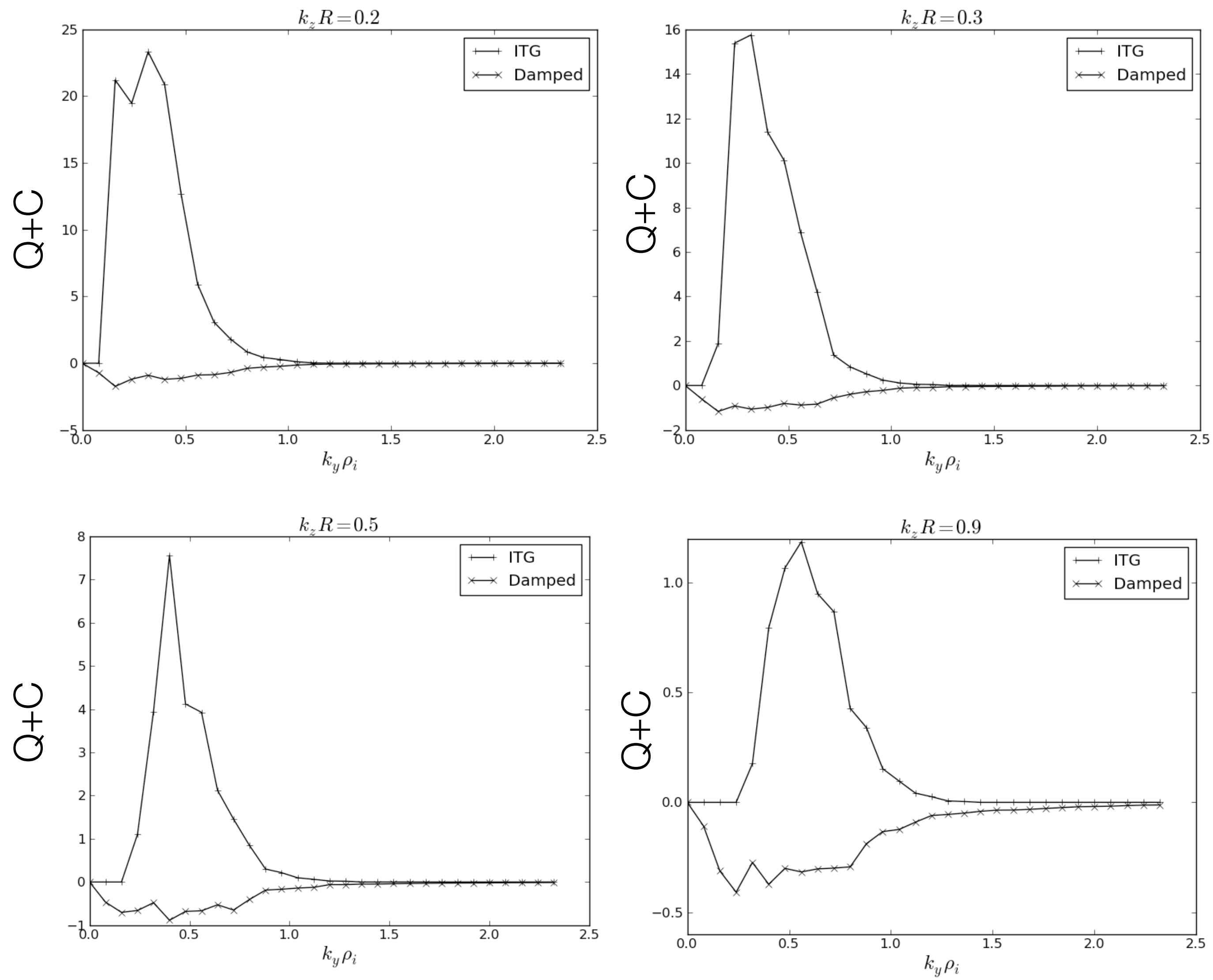

Significant **energy sink** from damped modes ==>**associated with small scales in neither k-space nor v-space**

High k Spectra

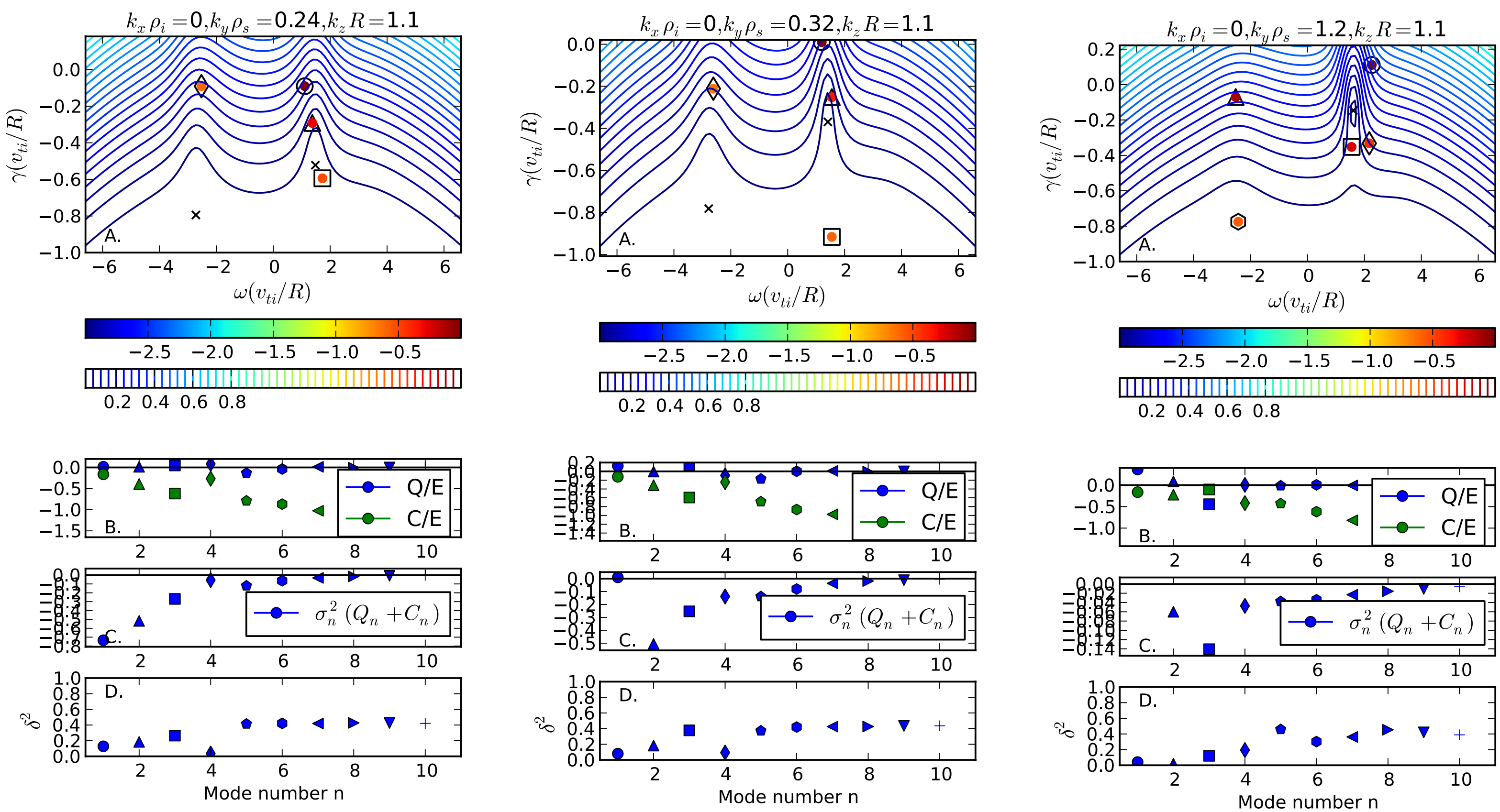

ITG and DW significantly less damped than linear
Also manifest in deformation of pseudospectra
Relevance for cascades in presence of Landau damping
May be connection with G. Plunk--Phys. Plasmas **20**, 032304 (2013).

Outline

- SVD-mathematical foundation
  - Orthogonality
  - Optimality
- **Examples**
  - Dynamo flows
  - Subdominant microtearing modes
  - Saturation via damped eigenmodes
- **Summary/Conclusions**

Summary Conclusions

- POD/SVD extracts optimal, orthogonal representation of turbulence fluctuations
- Examples
  - Dynamo—SVD identifies mode that suppresses dynamo
  - Electromagnetic gyrokinetic ITG simulations
    - Linearly stable microtearing mode responsible for magnetic stochasticity and transport
  - Damped eigenmodes—damped eigenmodes provide potent energy sink in region of energy drive.
    - Marginally stable drift wave and mode with negative Q identified in nonlinear spectrum
    - Negative Q mode absent from linear spectrum, but can be identified in pseudospectrum

References

- POD/SVD:
  - Berkooz, et al. Annu. Rev. Fluid. Mech., 1993.
  - Holmes et al., (1996) 'Turbulence, Coherent Structures, Dynamical Systems and Symmetry', New York: Cambridge University Press
- Dynamo+POD
  - Limone et al., PRE, 2013
- Electromagnetic gyrokinetic simulations and subdominant microtearing modes
  - Hatch et al., PRL, 2012, Hatch et al., PoP, 2013
- Damped eigenmodes as saturation mechanism
  - Fluid models: Terry et al., PoP, 2006
  - Gyrokinetics: Hatch et al. PRL 2011, PoP, 2012
- Higher Order Singular Value Decomposition (HOSVD)—high-dimensional generalization of SVD
  - Hatch et al., JCP, 2012
- Other recent plasma applications
  - Futatani et al., PoP, 2009
  - del-Castillo Negrete et al., JCP 2007, PoP 2008

Pseudospectra

"... even if all of the eigenvalues of a linear system are distinct and lie well inside the lower half plane, inputs to that system may be amplified by arbitrarily large factors if the eigenfunctions are not orthogonal to one another."

$$\Lambda_\epsilon(A) \;=\; \{\, z \in \mathbf{C} : \; \|(zI - A)^{-1}\| \geq \epsilon^{-1} \,\}$$

$$\Lambda_\epsilon(A) \;=\; \{\, z \in \mathbf{C} : \; \sigma_{\min}(zI - A) \leq \epsilon \,\}$$

Classic Example:

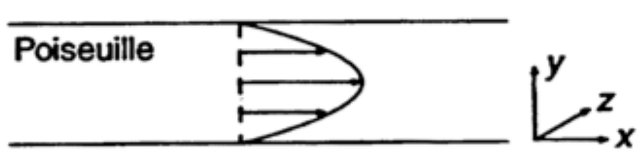

Trefethen-*Science*, New Series, Vol. 261, No. 5121. (Jul. 30, 1993), pp. 578-584.
Trefethen-SIAM REV. Vol. 39, No. 3, pp. 383–406, September 1997

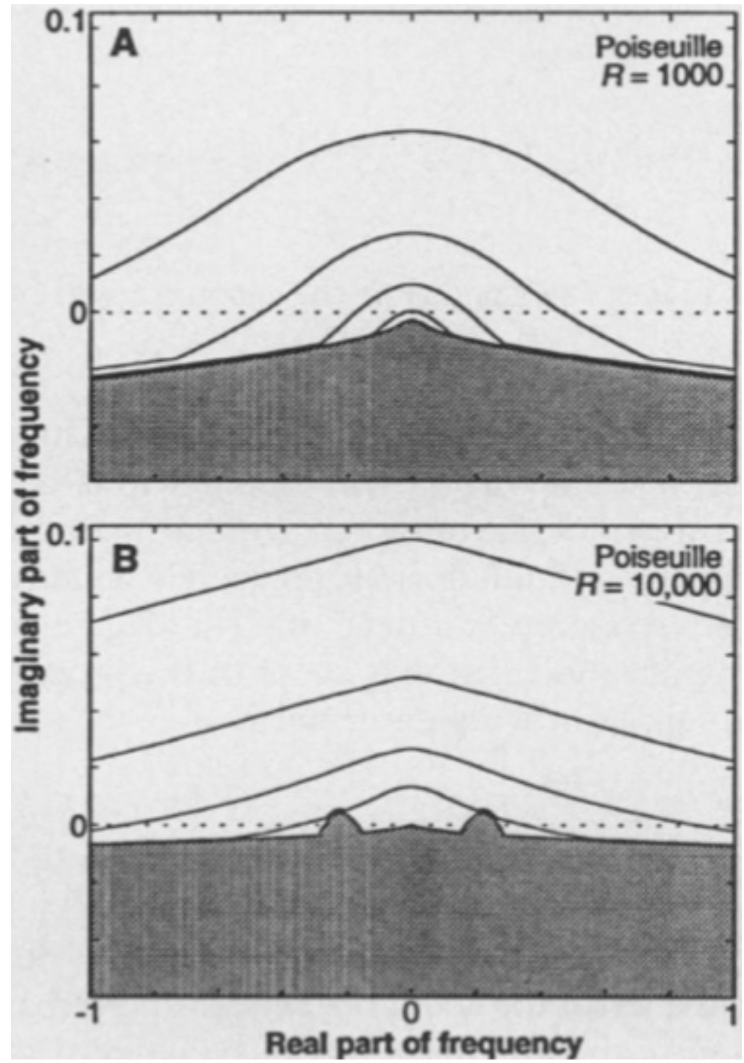

Hermite representation in GK

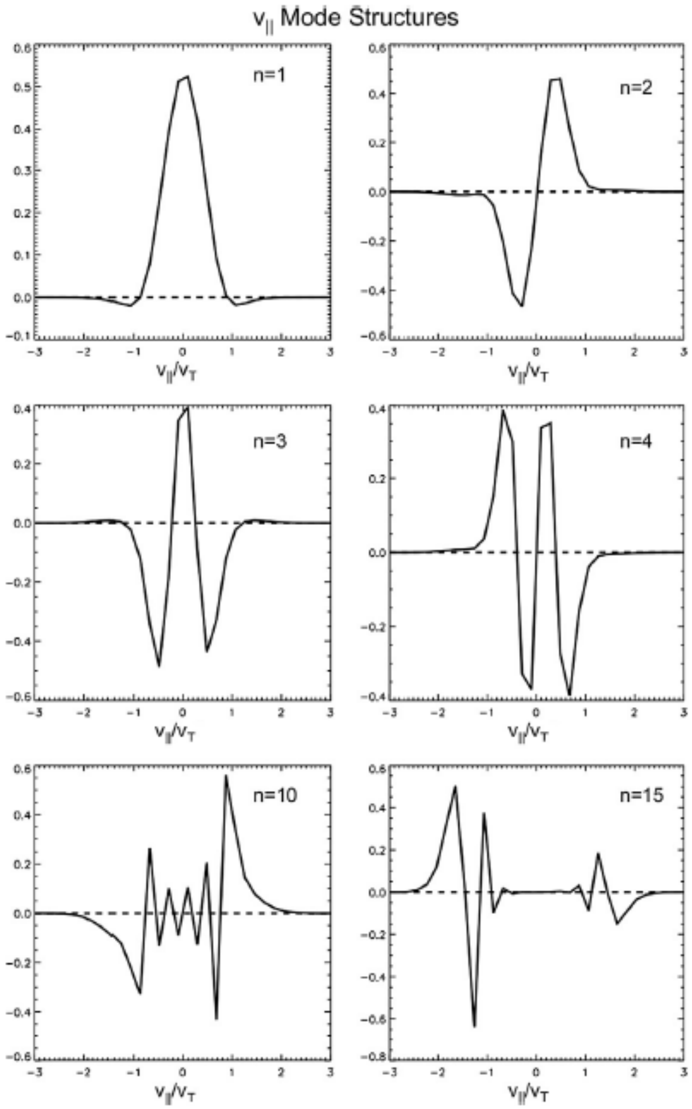

Higher order singular value decomposition (HOSVD) applied to 6D gyrokinetics (5D plus time)—extracts mode structures for each coordinate.

➔Hermite polynomials—natural representation of parallel velocity in GK

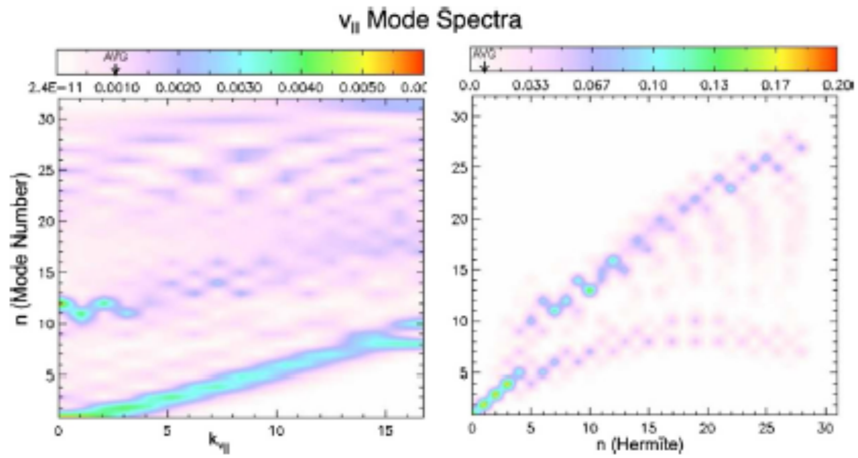

Fig. 9. Fourier (A) and Hermite (B) spectra of the HOSVD $v_{\parallel}$-modes.

Hatch et al. JCP '12

Energy Evolution

Electrostatic part:

$$\frac{\partial \varepsilon_{\boldsymbol{k}}^{(\phi)}}{\partial t} = J_{\boldsymbol{k}}^{(\phi)} + N_{\boldsymbol{k}}^{(\phi)} \qquad J_{\boldsymbol{k}}^{(\phi)} \equiv \Re\left[-ik_z\pi^{\frac{1}{4}}\bar{\phi}^*\hat{f}_{\boldsymbol{k},1}\right]$$

$$N_{\boldsymbol{k}}^{(\phi)} \equiv \Re\left[\sum_{\boldsymbol{k}'} T_{\boldsymbol{k},\boldsymbol{k}'}^{(\phi)}\right] \qquad T_{\boldsymbol{k},\boldsymbol{k}'}^{(\phi)} = \pi^{1/4}(k'_x k_y - k_x k'_y)\bar{\phi}_{\boldsymbol{k}}^*\bar{\phi}_{\boldsymbol{k}'}\hat{f}_{0,\boldsymbol{k}-\boldsymbol{k}'}$$

Entropy part:

$$\frac{\partial \varepsilon_{\boldsymbol{k},n}^{(f)}}{\partial t} = \eta_i Q_{\boldsymbol{k}}\delta_{n,2} - \nu n \varepsilon_{\boldsymbol{k},n}^{(f)} - J_{\boldsymbol{k}}^{(\phi)}\delta_{n,1} + J_{\boldsymbol{k},n-1/2} - J_{\boldsymbol{k},n+1/2} + N_{\boldsymbol{k}}^{(f)}$$

$$\eta_i Q = \Re\left[-\frac{\pi^{1/4}}{\sqrt{2}}\eta_i i k_y e^{-k_\perp^2/2}\hat{f}_2^*\phi\right]$$

$$J_{\boldsymbol{k},n-1/2} \equiv \Re\left[-\pi^{\frac{1}{2}} i k_z \sqrt{n}\hat{f}_{\boldsymbol{k},n}^*\hat{f}_{\boldsymbol{k},n-1}\right] \qquad J_{\boldsymbol{k},n+1/2} \equiv \Re\left[\pi^{\frac{1}{2}} i k_z \sqrt{n+1}\hat{f}_{\boldsymbol{k},n}^*\hat{f}_{\boldsymbol{k},n+1}\right]$$

$$N_{\boldsymbol{k},n}^{(f)} \equiv \Re\left[\sum_{\boldsymbol{k}'} T_{\boldsymbol{k},\boldsymbol{k}',n}^{(f)}\right] \qquad T_{\boldsymbol{k},\boldsymbol{k}',n}^{(f)} = -\pi^{1/2}(k'_x k_y - k_x k'_y)\hat{f}_{\boldsymbol{k},n}^*\bar{\phi}_{\boldsymbol{k}-\boldsymbol{k}'}\hat{f}_{\boldsymbol{k}',n}$$

SVD Compared to Linear Modes

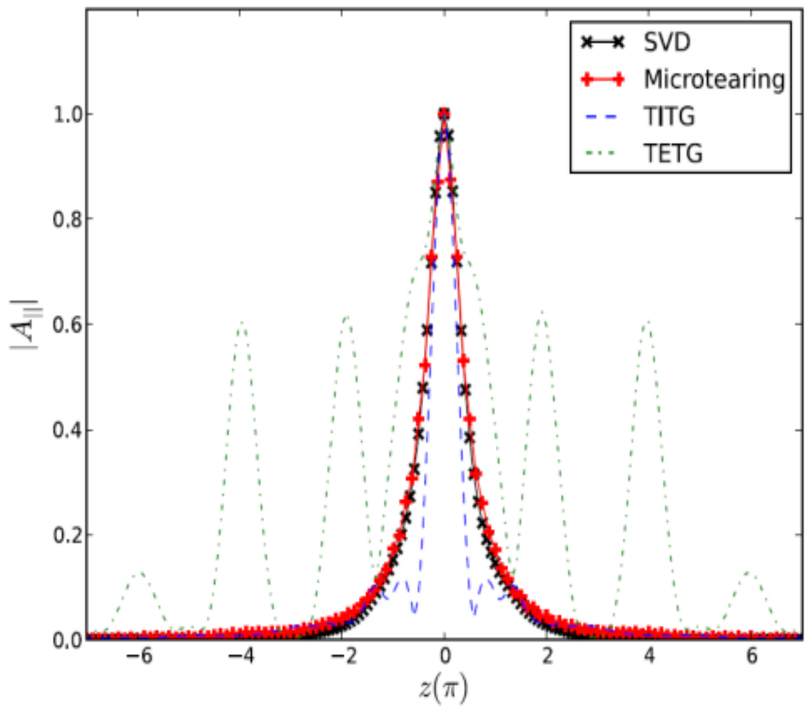

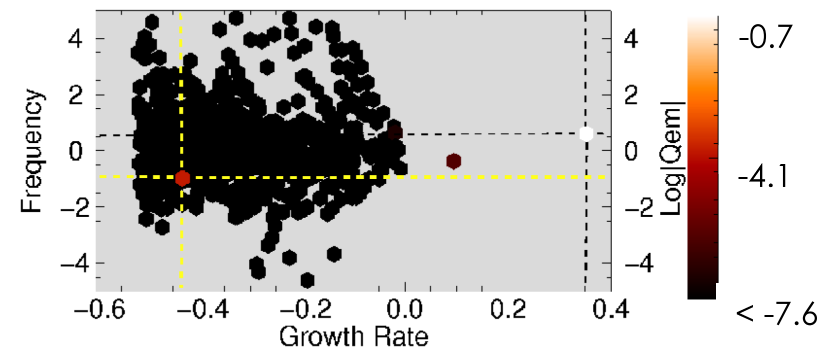

	TITG	TETG	MTM	SVD
$Q_e^{EM}/\lvert Q_i^{ES}\rvert$	4.8×10^{-3}	-0.13	730	330
$\int A_{\|}^2 dz / \int \Phi^2 dz$	1.3×10^{-3}	2.8×10^{-5}	0.10	0.16

Can compare POD mode with linear eigenmodes
➔Most important POD mode very similar to microtearing mode.

D.R. Hatch et al., PRL 2012., PoP 2013.

Schematic Energy Transfer

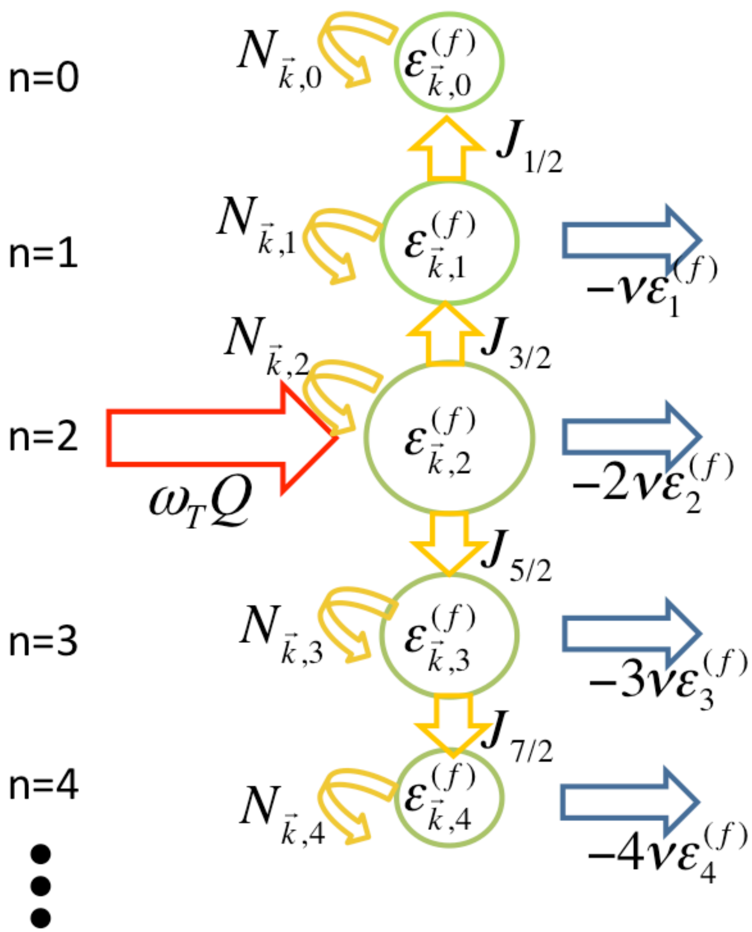

Free Energy

Free energy equations:

$$\varepsilon_{\boldsymbol{k},n} = \varepsilon^{(f)}_{\boldsymbol{k},n} + \varepsilon^{(\phi)}_{\boldsymbol{k}}\delta_{n,0}$$

$$\varepsilon^{(f)}_{\boldsymbol{k},n} \equiv \frac{1}{2}\pi^{\frac{1}{2}}|\hat{f}_{\boldsymbol{k},n}|^2$$

$$\varepsilon^{(\phi)}_{\boldsymbol{k}} \equiv \frac{1}{2D(k_\perp)}|\phi_{\boldsymbol{k}}|^2$$

Energy Evolution

Electrostatic part:

$$\frac{\partial \varepsilon_{\boldsymbol{k}}^{(\phi)}}{\partial t} = J_{\boldsymbol{k}}^{(\phi)} + N_{\boldsymbol{k}}^{(\phi)} \qquad J_{\boldsymbol{k}}^{(\phi)} \equiv \Re\left[-ik_z \pi^{\frac{1}{4}} \bar{\phi}^* \hat{f}_{\boldsymbol{k},1}\right]$$

$$N_{\boldsymbol{k}}^{(\phi)} \equiv \Re\left[\sum_{\boldsymbol{k}'} T_{\boldsymbol{k},\boldsymbol{k}'}^{(\phi)}\right] \qquad T_{\boldsymbol{k},\boldsymbol{k}'}^{(\phi)} = \pi^{1/4}(k_x' k_y - k_x k_y')\bar{\phi}_{\boldsymbol{k}}^* \bar{\phi}_{\boldsymbol{k}'} \hat{f}_{0,\boldsymbol{k}-\boldsymbol{k}'}$$

Entropy part:

$$\frac{\partial \varepsilon_{\boldsymbol{k},n}^{(f)}}{\partial t} = \eta_i Q_{\boldsymbol{k}} \delta_{n,2} - \nu n \varepsilon_{\boldsymbol{k},n}^{(f)} - J_{\boldsymbol{k}}^{(\phi)} \delta_{n,1} + J_{\boldsymbol{k},n-1/2} - J_{\boldsymbol{k},n+1/2} + N_{\boldsymbol{k}}^{(f)}$$

$$\eta_i Q = \Re\left[-\frac{\pi^{1/4}}{\sqrt{2}} \eta_i i k_y e^{-k_\perp^2/2} \hat{f}_2^* \phi\right]$$

$$J_{\boldsymbol{k},n-1/2} \equiv \Re\left[-\pi^{\frac{1}{2}} i k_z \sqrt{n} \hat{f}_{\boldsymbol{k},n}^* \hat{f}_{\boldsymbol{k},n-1}\right] \qquad J_{\boldsymbol{k},n+1/2} \equiv \Re\left[\pi^{\frac{1}{2}} i k_z \sqrt{n+1} \hat{f}_{\boldsymbol{k},n}^* \hat{f}_{\boldsymbol{k},n+1}\right]$$

$$N_{\boldsymbol{k},n}^{(f)} \equiv \Re\left[\sum_{\boldsymbol{k}'} T_{\boldsymbol{k},\boldsymbol{k}',n}^{(f)}\right] \qquad T_{\boldsymbol{k},\boldsymbol{k}',n}^{(f)} = -\pi^{1/2}(k_x' k_y - k_x k_y')\hat{f}_{\boldsymbol{k},n}^* \bar{\phi}_{\boldsymbol{k}-\boldsymbol{k}'} \hat{f}_{\boldsymbol{k}',n}$$